Easy synthesis and water solubility of ruthenium complexes containing PPh$_3$, mTPPMS, PTA and mPTA, (mTPPMS = *meta*-triphenyphosphine monosulfonate, PTA = 1,3,5-triaza-7-phosphaadamantane, mPTA = *N*-methyl-1,3,5-triaza-7-phosphaadamantane).

Manuel Serrano-Ruiz,[a] Pablo Lorenzo-Luis,[b,*] Antonio Romerosa[a,*]

[a] *Área de Química Inorgánica-CIESOL, Facultad de Ciencias, Universidad de Almería, Almería, Spain.*

[b] *Departamento de Química-Área de Inorgánica, Facultad de Química, Universidad de La Laguna, La Laguna, Tenerife, Spain*

Corresponding author. E-mail: romerosa@ual.es (A. Romerosa), plorenzo@ull.es (P. Lorenzo-Luis)

ABSTRACT

New water soluble {CpRu} complexes with formula [RuCpX(L^1)(L^2)]$^{n+}$ (L^1, L^2 = PPh$_3$, mTPPMS (*meta*-triphenyphsphine monosulfonate), PTA (1,3,5-triaza-7-phosphaadamantane), mPTA (*N*-methyl-1,3,5-triaza-7-phosphaadamantane)) were synthesized and characterized by elemental analytical, IR and NMR spectroscopy. Complexes [RuClCp(PPh$_3$)(mPTA)](OTf) (**3·OTf**), [RuCpI(PPh$_3$)(mPTA)]·2I·EtOH (**5·I·EtOH**)·and [RuCpBr(PTA)$_2$]·3.5H$_2$O (**6·3.5H$_2$O**) were also characterized by single crystal X-ray diffraction. The NMR spectra of the complexes are in agreement with their composition, indicating also that their solid state structure is maintained in solution. These results are integrated in a thorough overview of preparative routes, structural composition and solubility of {CpRu} complexes containing water-soluble phosphanes.

Keywords: Ruthenium, water soluble complexes, water soluble phosphanes.

1. Introduction

Pearson's hard-soft acid-base (HSAB) principle, introduced in 1963 [1] has become one of the central constructs of modern chemistry. The HSAB principle is useful in making qualitative estimates of the solubility of ionic salts in water and to some extent in other solvents, though not many other solvents yield solvation energies large enough to dissolve many ionic salts. In water solutions the H$_2$O oxygen atom is the electron donor that is strongly electronegative and therefore water is a hard base. As a general strategy aqua-soluble ligands are used to provide water solubility to metal complexes. Nevertheless, there is not an extensive study on complex solubility in water related with complex composition, structure and, number and nature of water-soluble ligands. Over the last years, we have published the synthesis of the piano-stool complexes [RuCp′X(L^1)(L^2)]$^{n+}$ (Cp′= Cp; Cp*; X = Cl, I, L^1 = PPh$_3$; L^2 = PTA, mPTA; L^1 = L^2 = PTA, mPTA), Na$_2$[RuCpX(mTPPMS)$_2$] (X = Cl, I) and Na$_x$[RuCp(mTPPMS)(PR$^1_3$)(PR$^2_3$)](OTf)$_y$ (PR$^1_3$ =

PR$^2_3$ = PPh$_3$, PTA, x = y = 0. PR$^1_3$ = mTPPMS, PR$^2_3$ = PTA, x = 1, y = 0. PR$^1_3$ = mTPPMS, PR$^2_3$ = mPTA, x = y = 0. PR$^1_3$ = PR$^2_3$ = mTPPMS, x = 2, y = 0. PR$^1_3$ = PPh$_3$, PR$^2_3$ = PTA, x = y = 0. PR$^1_3$ = mPTA, PR$^2_3$ = PPh$_3$, x = 0, y = 1) (mTPPMS = *meta*-triphenyphsphine monosulfonate; OTf = $^-$OSO$_2$CF$_3$; PTA = 1,3,5-triaza-7-phosphaadamantane; mPTA = *N*-methyl-PTA) and reported on their interaction with DNA [2,3,4]. These complexes constitute an entire family of {CpRu}-complexes with similar structure, which provide the possibility of correlating their composition with their solubility in water.

This paper describes the synthesis and characterization of new water soluble half-sandwich ruthenium(II) complexes with halides and/or other hydrophobic (PPh$_3$), amphiphilic (mTPPMS) and hydrophilic (PTA and mPTA) phosphane coligands needed to arrive to have a more complete overview about the relation between structure and water solubility of the complex family of general formula [RuCpX(L^1)(L^2)]$^{n+}$ (X = Cl, Br, I; L^1 = PPh$_3$; mTPPMS, L^2 = mPTA, PTA; L^1 = L^2 = PTA, mPTA).

2. Experimental

2.1. Materials and methods

All reagents and chemicals were reagent grade and, unless otherwise stated, were used as received by commercial suppliers. All reactions and manipulations were routinely performed under a dry nitrogen atmosphere. The solid complexes were collected on sintered glass-frits and purified as described. The aryl-sulfonated (mTPPMS) and the cage-like phosphines (PTA and mPTA) as well as the complexes [RuClCp(PPh$_3$)$_2$], Na$_2$[RuClCp(mTPPMS)$_2$], [RuClCp(PPh$_3$)(mPTA)](OTf) (**3·OTf**), [RuClCp(PPh$_3$)(PTA)] and [RuClCp(PTA)$_2$], were prepared as described in the literature [2,3,4,5].

The deuterated solvents CD₃OD, DMSO-d₆ and CDCl₃ (Cortec-Euriso-top) was dried over molecular sieves (0.4 nm). ^{1}H and ^{13}C{^{1}H} NMR spectra were recorded on a Bruker DRX300 spectrometers operating at 300.13 MHz (^{1}H) and 75.47 MHz (^{13}C), respectively. Peak positions are relative to tetramethylsilane and were calibrated against the residual solvent resonance (^{1}H) or the deuterated solvent multiplet (^{13}C). ^{31}P{^{1}H} and ^{19}F{^{1}H} NMR spectra were recorded on the same instruments operating at 121.49 and 282.40 MHz. The chemical shifts were measured relative to external 85% H₃PO₄ and CFCl₃ with downfield values taken as positive. Infrared spectra were recorded on KBr disks using an IR-ATI Mattson Infinity Series. Elemental analysis (C, H, N, S) were performed on a Fisons Instruments EA 1108 elemental analyser.

2.2. Synthesis of Na[RuCp(mTPPMS)₂(PPh₃)]·(1)

To an ethanolic solution of Na₂[RuClCp(mTPPMS)₂] [4] (0.36 g, 0.39 mmol) was added gradually NaBF₄ (0.04 g, 0.37 mmol). The reaction mixture was sonicated 30 min. giving rise a white precipitate, which was filtered. Then PPh₃ (0.097 g, 0.37 mmol) was added to the yellow solution and the mixture was refluxed for 5 min. The resulting solution was concentrated until 0.5 cm3 and the resulting yellow precipitate filtered, washed with EtO₂ (3 x 2 cm3) and dried under vacuum. Powder yield: 0.28 g, 63 %. S_{25}(mg/cm^3): 8.3. *Anal.* Calc. (C₅₉H₄₈NaO₆P₃RuS₂) (1134.13): C, 62.5; H, 4.3; S, 5.6%. Found C, 60.9; H; 4.0, S, 5.3%. FT-IR (KBr, cm^{-1}) 1185 and 1222 for ν (SO₃). ^{1}H NMR (300.13 MHz, 20 ºC, SiMe₄, CD₃OD): δ(ppm) 4.15 (bm, Cp, 5 H), 7.13 - 8.17 (m, aromatic, 43 H); ^{13}C{^{1}H} NMR (75.47 MHz, 20 ºC, SiMe₄, CD₃OD): δ(ppm) 81.18 (bm, Cp), 126.19 – 145.73 (m, aromatic); ^{31}P{^{1}H} NMR (121.49, 20 ºC, 85% H₃PO₄, CD₃OD): δ(ppm) 39.60 (AXY system, $^1J_{(PPh_3/mTPPMS)}$ = 49.9 Hz, $^1J_{(PPh_3/mTPPMS)}$ = 46.2 Hz, PPh₃); 39.80 (bd, $^1J_{(mTPPMS/PPh_3)}$ = 46.2 Hz, mTPPMS).

2.3. Synthesis of [RuCp(PPh₃)₂(mPTA)](OTf)(BF₄) (2·OTf·BF₄)

The complex [RuClCp(PPh₃)₂] [2] (0.29 g, 0.40 mmol), mPTA(OSO₂CF₃) (0.145 g, 0.45 mmol) and NaBF₄ (0.049 g, 0.45 mmol) were introduced into a vessel containing 50 cm3 of EtOH. The resulting mixture was kept at refluxing temperature for 12 hours and evaporated under vacuum until 10 cm3. The obtained yellow precipitate was filtered, washed with Et₂O (2 x 5 cm3) and vacuum dried. Powder yield: 0.332 g, 75 %. S_{25}(mg/cm^3): 2.7. *Anal.* Calc. (C₄₉H₅₀N₃P₃RuSO₃BF₇) (1098.81): C, 53.1; H, 4.6; N, 3.8; S, 2.9 %. Found C, 51.9; H, 4.3; N,3.6; S, 3.6%. FT-IR (KBr, cm^{-1}) 1253 and 1273 for ν (OSO). ^{1}H NMR

(300.13 MHz, 20 ºC, SiMe₄, CDCl₃): δ(ppm) 2.87 (s, CH₃N, 3 H), 2.89 (ABX system, $^2J_{HH}$ = 1.8 Hz, $^2J_{HP}$ = 8.34 Hz, CH₃NCHP, 2H), 3.51 (ABX system, $^2J_{HH}$ = 6.18 Hz, $^2J_{HP}$ = 15.07 Hz, PCH₂N, 2 H), 3.81 – 4.39 (m, CH₃NCH₂N, 4 H), 4.66 - 5.01 (m, NCH₂N, 2 H), 5.13 (s, Cp, 5 H), 7.09 – 7.66 (m, aromatic, 30 H); ^{13}C{^{1}H} NMR (75.47 MHz, 20 ºC, SiMe₄, D₂O): δ(ppm) 48.66 (s, CH₃N), 51.85 (d, $^1J_{CP}$ = 13.81 Hz, PCH₂N), 60.90 (d, $^1J_{CP}$ = 10.21 Hz, PCH₂NCH₃), 68.52 (d, $^3J_{CP}$ = 6.0 NCH₂N), 79.65 (d, $^3J_{CP}$ = 3.61 Hz, NCH₂NCH₃), 85.93 (s, Cp), 128.95 – 136.54 (aromatic, PPh₃); ^{31}P{^{1}H} NMR (121.49, 20 ºC, 85% H₃PO₄, CDCl₃): δ(ppm) -25.48 (t, $^2J_{PP}$ = 39.6 Hz, mPTA), 39.33 (d, $^2J_{PP}$ = 40.35 Hz, , PPh₃, 2 P); ^{19}F{^{1}H} NMR (282.40, 20 ºC, CFCl₃, D₂O): δ(ppm) -78.98 (s, $^-$OTf), δ(ppm) -150.19 (s, BF₄$^-$).

2.4. Synthesis of [RuCpCl(PPh₃)(mPTA)](OTf) (3·OTf)

Complex **3·OTf** was prepared by following the method reported by us [3]. The conditions to obtain this complex were optimized and crystals suitable for X-ray diffraction were grown by slow evaporation from a solution of **3·OTf** in CHCl₃/n-hexane (1:1) (synthesis in Scheme 1 and X-ray structure in Fig. 2). Crystal data and structure refinement information are listed in Table 1.

2.5. Synthesis of [RuCp(PPh₃)(PTA)(mPTA)](OTf)(Cl) (4·OTf·Cl)

A solution of mPTA(OSO₂CF₃) (0.1 g, 0.32 mmol) in 2 cm3 of MeOH was added to [RuClCp(PPh₃)(PTA)] [4] (0.2 g, 0.32 mmol) previously dissolved in 3 cm3 of MeOH. The mixture was stirred for 15 minutes at room temperature then to refluxing temperature. After 1 hour the yellow solution was slowly cooled at room temperature and yellow-orange microcrystals were obtained, which were filtered and dried under an argon flow. Powder yield: 0.18 g, 90 %. S_{25}(mg/cm^3): 0.4. *Anal.* Calc. (C₃₇H₄₇ClN₆P₃RuSO₃F₃) (942.32): C, 47.2; H, 5.0; N, 8.9; S, 3.4. Found: C, 48.5; H, 5.1; N, 9.1; S, 3.4%. FT-IR (KBr, cm^{-1}) 1196 for ν (SO₃). ^{1}H NMR (300.13 MHz, 20 ºC, SiMe₄, CD₃OD): δ(ppm) 2.82 (bs, CH₃N$_{mPTA}$, 3 H), 3.62 – 4.00 (m, CH₂P$_{PTA}$ + CH₂P$_{mPTA}$, 10 H), 4.16 – 4.59 (m, CH₂N$_{PTA}$ + CH₂N$_{mPTA}$, 8 H), 3.77 - 5.13 (m, CH₂N$_{mPTA}$ + CH₂P$_{mPTA}$, 6 H), 5.25 (s, Cp, 5 H), 7.31 – 7.64 (m, aromatic protons, 15 H); ^{13}C{^{1}H} NMR (75.47 MHz, 20 ºC, SiMe₄, CD₃OD): δ(ppm) 53.07 (s, CH₃(mPTA)-N), 56.60 (m, CP$_{PTA}$), 56.80 (m, CP$_{mPTA}$), 61.50 (d, $^1J_{CP}$ = 3.6 Hz, CH₃NCP$_{mPTA}$), 71.41, 71.46 (m, NCN$_{PTA}$ + NCN$_{mPTA}$), 79.86 (m, CH₃NCN$_{mPTA}$), 84.20 (bs, Cp), 129.03 – 136.16 (m, PPh₃); ^{31}P{^{1}H} NMR (121.49, 20 ºC, 85% H₃PO₄, DMSO): δ(ppm) -39.40 (AMX system, $^1J_{(PTA/mPTA)}$ = 35.4 Hz, $^1J_{(PTA/PPh_3)}$ = 36.0 Hz, PTA), -16.18 (AMX system, $^1J_{(mPTA/mPTA)}$ = 35.4

Hz, $^1J_{(mPTA/PPh_3)}$ = 35.3 Hz, mPTA), 47.22 (AMX system, $^1J_{(PPh_3/PTA)}$ = 35.3 Hz, $^1J_{(PPh_3/mPTA)}$ = 36.0 Hz, PPh$_3$), ^{19}F{^{1}H} NMR (282.40, 20 ºC, CFCl$_3$, MeOH): δ (ppm) -78.98 (s, OTf).

2.6. Synthesis of [RuCpI(PPh₃)(mPTA)]·I·EtOH (5·I·EtOH)·

Complex **5·I·EtOH** was prepared by reaction of **3·OTf** with NaI in refluxing EtOH by slight modification of the method previously published by us [3]. Powder yield: 0.105 g (45 %). S$_{25}$(mg/cm^3): ≤ 0.1 mg/cm^3. *Anal.* Calc. (C$_{32}$H$_{41}$I$_2$N$_3$P$_2$RuO) (900.53): C, 42.7; H, 4.6; N, 4.7. Found C, 42.5; H; 4.0, N, 4.1%. Crystals were undertaken by slow evaporation from EtOH/NaI (1:1.5).

2.7. Synthesis of [RuCpBr(PTA)₂]·3.5H₂O (6·3.5H₂O)

A solution of [RuCpCl(PTA)$_2$] [2,5] (0.10 g, 0,14 mmol) in 20 cm3 of MeOH was reacted with KBr (0.025 g, 0,21 mmol). The mixture refluxed for 4 hours, cooled down to room temperature and concentrated under reduced pressure to dryness. Addition of 10 cm3 of hot CH$_3$Cl with strong stirring afforded a yellow precipitate that was filtered, washed with Et$_2$O (3 x 3 cm3) and vacuum dried. Slow evaporation in water solution enabled obtaining crystals of good quality (X-ray structure in Fig. 4). Crystal data and structure refinement information are listed in Table 1. Power yield: 0.035 g, 81%. S$_{25}$(mg/cm^3): 30. *Anal.* Calc. (C$_{17}$H$_{36}$BrN$_6$P$_2$RuO$_{3.5}$) (623.44): C, 32.7; H, 5.8; N, 13.5. Found: C, 31.9; H, 5.4; N, 13.1.% ^{1}H NMR (300,13 MHz, D$_2$O, 20 º C): δ(ppm) 3.97 (ABX system, $^2J_{HH}$ = 15.0 Hz, $^2J_{HP}$ = 15.0 Hz, NCH$_2$P, 6H), 4.46 (bs, NCH$_2$N, 6H), 4.66 (s, Cp, 5H); ^{13}C{^{1}H} NMR (75.47 MHz, D$_2$O, 20 º C): δ(ppm) 54.80 (t, $^1J_{CP}$ = 9.0 Hz, NCH$_2$P), 70.56 (t, $^3J_{CP}$ = 3.0 Hz, NCH$_2$N), 77.01 (t, $^3J_{CP}$ = 1.8 Hz, Cp). ^{31}P{^{1}H} NMR (121.49 Mz, D$_2$O, 20º C): δ(ppm) -26.37 (s, PTA).

2.8. Synthesis of [RuCp(PTA)₂(mPTA)](OTf)·(Cl) (7·OTf·Cl)

Into a vessel the complex [RuClCp(PTA)$_2$] [2,5] (0.1 g, 0.19 mmol), mPTA(OSO$_2$CF$_3$) (0.06 g, 0.19 mmol) and 15 cm3 of MeOH were introduced. The mixture was kept at refluxing temperature for 1 day. The resulting pale-yellow precipitate was filtered, washed with MeOH (2 x 3 cm3), Et$_2$O (2 x 2 cm3) and vacuum dried. Powder yield: 0.09 g, 57%. S$_{25}$(mg/cm^3): 200. *Anal.* Calc. (C$_{25}$H$_{44}$ClN$_9$P$_3$RuSO$_3$F$_3$) (837.18): C, 35.9; H, 5.3; N, 15.1; S, 3.8%. Found: C, 36.2; H, 5.5; N, 15.0; S, 4.0%. FT-IR (KBr, cm^{-1}) 1244, 1258 and 1280 for ν (SO$_3$). ^{1}H NMR (300.13 MHz, 20 ºC, SiMe$_4$, D$_2$O):δ(ppm) 2.82 (bd, $^4J_{HP}$ = 1.8 Hz, CH$_3$N$_{mPTA}$N, 3

H), 3.94 (ABX system, $^2J_{HH}$ = 13.7 Hz, $^2J_{HP}$ = 45.9 Hz, PCH$_2$N$_{mPTA}$, 4 H), 4.27 (bs, CH$_3$NCH$_2$P$_{mPTA}$, 2 H), 4.34 – 4.50 (m, NCH$_2$N$_{PTA}$, 6 H), 4.54 – 4.63 (2d, $^1J_{HH}$ = 13.7 Hz, NCH$_2$N$_{mPTA}$, 2 H), 4.88 – 5.10 (m, CH$_3$NCH$_2$N$_{mPTA}$, 4 H); 5.26 (s, Cp, 5 H); ^{13}C{^{1}H} NMR (75.47 MHz, 20 ºC, SiMe$_4$, D$_2$O): δ(ppm) 48.82 (s, CH$_3$N$_{mPTA}$), 54.49 (d, $^1J_{CP}$ = 17.3 Hz, PCH$_2$N$_{mPTA}$), 56.87 (d, $^1J_{CP}$ = 9.7 Hz, PCH$_2$N$_{PTA}$), 62.07-62.27 (m, CH$_3$PCH$_2$N$_{mPTA}$), 68.58 -68.66 (m, NCH$_2$N$_{mPTA}$), 70.40 (s, NCH$_2$N$_{PTA}$), 79.87 (s, CH$_3$NCH$_2$N$_{mPTA}$), 82.93 (s, Cp); ^{31}P{^{1}H} NMR (121.49, 20 ºC, 85% H$_3$PO$_4$, D$_2$O): δ(ppm) -25.97 (d, $^2J_{PTA/mPTA}$ = 35.4 Hz, PTA), -8.6 (t, $^2J_{mPTA/PTA}$ = 35.4 Hz, mPTA). ^{19}F{^{1}H} NMR (282.40, 20 ºC, CFCl$_3$, D$_2$O): δ(ppm) -78.98 (s, OTf).

2.9. Synthesis of [RuCp(PTA)₃](BF₄) (8·BF₄)

The ligand PTA (0.03 g, 0.191 mmol) and NaBF$_4$ (0.11 g, 0.193 mmol) were added to a suspension of [RuClCp(PTA)$_2$] [2,5] (0.10 g, 0.193 mmol) in 15 cm3 of MeOH. The mixture was stirred at room temperature for 10 minutes and kept to refluxing temperature for 10 hours. The resulting pale yellow precipitate was filtered, washed with MeOH (2 x 5 cm3) and Et$_2$O (2 x 5 cm3), vacuum dried and then dissolved in 30 cm3 of CHCl$_3$. The obtained suspension was filtered out and evaporated under vacuum until 1 cm3. Addition of 5 cm3 of Et$_2$OH afforded a pale yellow precipitate that was filtered out, washed with Et$_2$O (2 x 2 cm3) and vacuum dried. Powder yield: 0.070 g, 51 %. S$_{25}$(mg/cm^3): 40. *Anal.* Calc. (C$_{23}$H$_{41}$N$_9$P$_3$RuBF$_4$) (724.44): C, 38.1; H, 5.7; N, 17.4. Found: C, 37.8; H, 5.5; N, 16.9%. ^{1}H NMR (300.13 MHz, 20 ºC, SiMe$_4$, D$_2$O): δ(ppm) 3.97 (bs, NCH$_2$P$_{PTA}$, 18 H), 4.48 – 4.60 (m, NCH$_2$N$_{PTA}$, 18 H), 4.70 (s, Cp, 5 H); ^{13}C{^{1}H} NMR (75.47 MHz, 20 ºC, SiMe$_4$, D$_2$O): δ(ppm) 56.92 (AXY system, $^1J_{CP}$ = 8.6 Hz, $^1J_{CH}$ = 8.6 Hz, NCH$_2$P$_{PTA}$), 70.43 (s, NCH$_2$N$_{PTA}$), 82.36 (s, Cp); ^{31}P{^{1}H} NMR (121.49, 20 ºC, 85% H$_3$PO$_4$, D$_2$O): δ(ppm) -24.09 (s, PTA). ^{19}F{^{1}H} NMR (282.40, 20 ºC, CFCl$_3$, D$_2$O): δ (ppm) -150.19 (s, BF$_4$).

2.10. X-ray structure determinations

X-ray diffraction data for **3·OTf**, **5·I·EtOH** and **6·3.5H₂O** were collected by φ-ω-scans technique on a Bruker APEX diffractometer using a graphite-monochromated MoK$_α$ radiation. The structures were solved by direct methods with SHELXS [6] and refined with full-matrix least-squares techniques on F^2 with SHELXL [6]. The C-bonded hydrogen atoms were included in idealized geometry riding on their parent atoms with C-H = 0.93-0.99 Å. The triflate anion (OTf = $^-$OSO$_2$CF$_3$) for **3·OTf**, was found to be disordered and refined isotropically, with Uiso(F1T/F2T) = 0.33 and 0.63; Uiso(F3T/F4T) = 0.72 and 0.28 and Uiso(F5T/F6T) = 0.79 and 0.21.

The ethanol molecule in **5·I·EtOH** is disordered between two positions with occupancy factors of $U\text{iso}(C1E/C2E) = 0.81$ and 0.21 and $U\text{iso}(C3E/C4E) = 0.61$ and 0.41. The water molecules for **6·3.5H₂O** were refined anisotropically, with $U\text{ani}(Ow4) = 0.5$. A brief summary of crystallographic details is given in Table 1.

Table 1. Crystal data and structure refinement information for complexes **3·OTf**, **5·I·EtOH** and **6·3.5H₂O**

	3·OTf	5·I·EtOH	6·3.5H₂O
Empirical formula	$C_{31}H_{35}ClN_3P_2RuO_3SF_3$	$C_{32}H_{35}I_2N_3P_2RuO$	$C_{17}H_{36}BrN_6P_2RuO_{3.5}$
Formula weight	785.14	894.44	623.44
Crystal system	triclinic	triclinic	monoclinic
Space group	P-1	P-1	P1 21/c 1
a (Å)	9.073(4)	9.4749(4)	11.8703(6)
b (Å)	13.535(5)	13.6140(6)	14.6036(7)
c (Å)	14.167(6)	14.0751(6)	14.1137(7)
α (°)	76.099(6)	89.8630(10)	90
β (°)	79.343(9)	72.3720(10)	107.6830(10)
γ (°)	78.203(7)	76.6490(10)	90
V(Å³)	1636.2(11)	1679.08(13)	2331.0(2)
Z	2	2	4
Calculated density (g·cm⁻³)	1.594	1.769	1.756
λ (Å)	0.71073	0.71069	0.71069
Absorption coefficient (mm⁻¹)	0.777	2.430	2.558
F(000)	800	872	1240
Data/restraints/parameters	4644/0/404	5846/0/369	4098 /0/280
Final R indices [I>2σ(I)]	$R_1 = 0.0745$; $wR_2 = 0.1497$	$R_1 = 0.0308$; $wR_2 = 0.0792$	$R_1 = 0.0493$; $wR_2 = 0.0910$
wR₂ R indices (all data)	$R_1 = 0.1236$; $wR_2 = 0.1725$	$R_1 = 0.0342$; $wR_2 = 0.0811$	$R_1 = 0.0662$; $wR_2 = 0.0965$
Goodness of fit (GOF) on F²	0.998	1.058	1.067
Largest difference in peak and hole (e·Å⁻³)	1.079 and -0.893	1.132 and -0.562	1.04 d -0.785

# 3. Results and discussion

3.1. Synthesis and characterization

One of the most popular synthetic routes to obtain aqueous organometallic complexes is the incorporation of water-soluble phosphines within the metal coordination sphere. A wide variety of functionalized aqua-soluble phosphines are actually known and their effectiveness in the aqueous organometallic chemistry context used [2-5].

We have synthesized a series of {CpRu} complexes of general formula $[RuCpX(L^1)(L^2)]^{n+}$ (X = Cl, Br, I; L^1 = PPh₃; mTPPMS, L^2 = mPTA, PTA; $L^1 = L^2$ = PTA, mPTA) (Table 2) that constitute an entire family with the same piano-stool structure in which three coordination positions on the Ru are occupied by the Cp and remaining the coordination positions available for being occupied by different ligands.

The steric and electronic properties of the benchmark ligand PPh₃ have a large effect on their poor solubility in water as far the bulky aryl ring of PPh₃ (cone angle $\theta = 145°$) causes a severe reduction on the water-solubility of the complexes (*vide infra*) [3]. In contrast, its *meta*-sulfonated derivative, the mTPPMS, display a large cone angle ($\theta = 151°$) [7] but also a much more larger solubility in water ($S_{(H_2O)20°C} = 80$ mg/cm³) and behaves like an amphiphile, [8] providing a significant water solubility to its metal complexes.

The small (cone angle $\theta \sim 103°$) cage-like phosphine PTA (Fig. 1) is largely soluble in water ($S_{(H_2O)25°C} = 235$ mg/cm³) but also in most of the organic solvents such as CHCl₃. The PTA derivatives and its metal complexes use to be also water soluble. The mPTA, the PTA mono-methylated derivative, is also largely soluble in water ($S_{(H_2O)25°C} = 240$ mg/cm³) [3],[9], displaying a similar cone angle to value than the PTA.
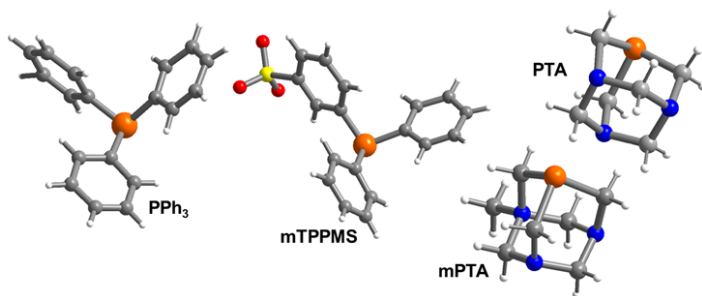
Fig 1. Combination of phosphines to provide control over the water-solubility of the family of complexes with formula [RuCpX(L^1)(L^2)]$^{n+}$ (X = Cl, Br, I; L^1 = PPh$_3$; mTPPMS, L^2 = mPTA, PTA; L^1 = L^2 = PTA, mPTA).

Table 2. Solubility (mg/cm^3) in water at 25 ºC.

Complex	S$_{(H_2O)25 ºC}$	Ref.
Na$_2$[RuCpCl(mTPPMS)$_2$]	41.0	[4]
Na$_2$[RuCp(mTPPMS)$_3$]	20.0	[4]
[RuCp(mTPPMS)(PPh$_3$)$_2$]	0.9	[4]
Na[RuCp(mTPPMS)$_2$(PPh$_3$)] (**1**)	8.3	
[RuCp(PPh$_3$)$_2$(mPTA)](OTf)(BF$_4$) (**2·OTf·BF$_4$**)	2.7	
[RuCpCl(PPh$_3$)(mPTA)]·(OTf) (**3·OTf**)	1.1	[3]
[RuCp(PPh$_3$)(PTA)(mPTA)](OTf)(Cl) (**4·OTf·Cl**)	0.4	
[RuCpI(PPh$_3$)(mPTA)]·I·EtOH (**5·I·EtOH**)	≤ 0.1	
[RuCpI(PPh$_3$)(mPTA)]·Cl	0.4	[3]
[RuCpI(PPh$_3$)(mPTA)]·(OSO$_2$CF$_3$)·2H$_2$O	≤ 0.1	[3]
[RuCpCl(mPTA)$_2$]·(OSO$_2$CF$_3$)$_2$	16	[10]
[RuCpCl(mPTA)$_2$]·(BF$_4$)$_2$	0.29*	[10]
[RuCpI(mPTA)$_2$]·(OSO$_2$CF$_3$)$_2$	32	[3]
[RuClCp(PTA)$_2$]	40	[2,5]
[RuCp*Cl(PTA)$_2$]	25	[2]
[RuCpBr(PTA)$_2$] (**6·3.5H$_2$O**)	30	
[RuCpI(PTA)$_2$]	10	[3]
[RuClCp(HPTA)$_2$]Cl$_2$·2H$_2$O	320	[11]
[RuCp(PTA)$_2$(mPTA)](OTf)(Cl) (**7·OTf·Cl**)	200	
[RuCp(PTA)$_3$](BF$_4$) (**8·BF$_4$**)	40	

OTf = $^-$OSO$_2$CF$_3$

* Solubility in water at 22 ºC
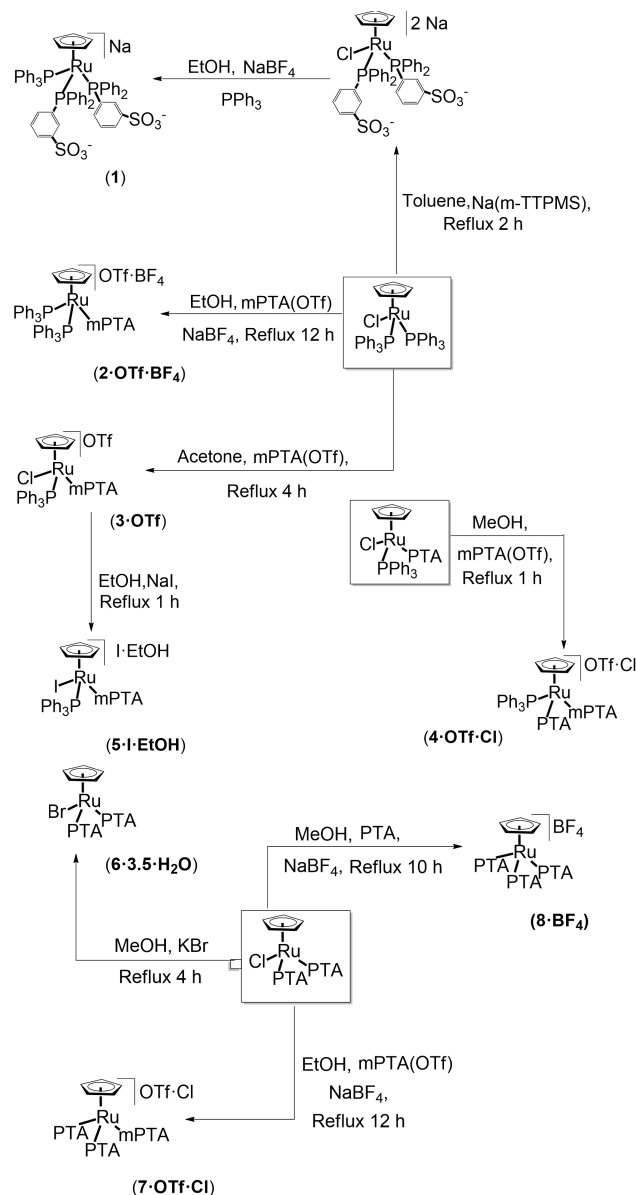
Scheme 1. Synthetic pathway for the family of organoruthenium complexes (PPh$_3$; mTPPMS = *meta*-triphenyphsphine monosulfonate; PTA = 1,3,5-triaza-7-phosphaadamantane and mPTA = *N*-methyl-PTA); OTf = $^-$OSO$_2$CF$_3$.

Most of the complexes in this paper (**2·OTf·BF$_4$**, **4·OTf·Cl**, as well as **6·3.5H$_2$O**, **7·OTf·Cl** and **8·BF$_4$**) were obtained by substitution of the Cl and PPh$_3$ ligands in the complexes [RuCl(PPh$_3$)$_2$], [RuCl(PPh$_3$)(PTA)] and [RuCl(PTA)$_2$] [2,3,5]. Complexes **1** and **5·I·EtOH** were obtained respectively from the complexes Na$_2$[RuClCp(*m*TPPMS)$_2$] [4] and [RuCpCl(PPh$_3$)(mPTA)](OTf) (**3·OTf**) [3], as the direct synthesis from the starting compound was not possible (Scheme 1).

Our research team prepared over the past few years some piano-stool water-soluble ruthenium complexes containing mTPPMS [4]. These complexes showed good solubility in water, which was related to the phosphanes coordinated to the metal.

The complex [RuCp(mTPPMS)(PPh$_3$)$_2$] was found to be practically insoluble in water ($S_{(H_2O)25°C}$ = 0.9 mg/cm^3) while the Na$_2$[RuCp(mTPPMS)$_3$] ($S_{(H_2O)25°C}$ = 20.0 mg/cm^3) showed a significant solubility but lower than that for Na$_2$[RuCpCl(mTPPMS)$_2$] ($S_{(H_2O)25°C}$ = 41 mg/cm^3). The scarce water solubility of [RuCp(mTPPMS)(PPh$_3$)$_2$] denotes the strong negative effect on the water solubility of the PPh$_3$ ligand (Table 2).

With this precedent, we decided to investigate the reaction of sulfonated phosphane precursor Na$_2$[RuCpCl(mTPPMS)$_2$] [4], with NaBF$_4$ and PPh$_3$ in ethanol (Scheme 1) to obtain the new complex Na[RuCp(mTPPMS)$_2$(PPh$_3$)] (**1**), which was isolated in moderate good yield (75%) and characterized by means of standard spectroscopic techniques as well as elemental analysis. The chemical shift in its ^{31}P{^{1}H} NMR spectrum of the mTPPMS ligands (39.80 ppm) moves *ca* 0.3 ppm to up-field from that observed for starting complex Na$_2$[RuCpCl(mTPPMS)$_2$] while the chemical shift of Cp in its ^{1}H NMR is closer (4.15 ppm) to that in starting complex (4.21 ppm) [4].

As expected the water solubility of **1** is larger than that for [RuCp(mTPPMS)(PPh$_3$)$_2$] with only one mTPPMS and two PPh$_3$, but lower than that for Na$_2$[RuCp(mTPPMS)$_3$] containing three mTPPMS ligands (Table 2). Therefore, we might infer that the steric and electronic properties cannot be regarded as separated factors without influence on the complex water-solubility (*vide infra*) [7].

Upon reaction of [RuClCp(PPh$_3$)$_2$] [2] with mPTA(OTf) and NaBF$_4$ the new complex [RuCp(PPh$_3$)$_2$(mPTA)](OTf)(BF$_4$) (**2·OTf·BF$_4$**) was obtained by exchanging the Cl coordinated to the metal by a mPTA ligand (Scheme 1). Its proposed structure was supported by the appearance in the ^{31}P{^{1}H} NMR of a doublet at 39.33 ppm for the PPh$_3$ and a triplet at -25.48 ppm for the mPTA. Additionally, its ^{1}H NMR spectrum shows signals at 2.87 ppm that only can be due to the group CH$_3$N$_{mPTA}$ [3]. It is important to point out that the ^{19}F{^{1}H} NMR spectrum shows for the CF$_3$ singlets at -78.98 ppm and for the BF$_4$ at -150.19 ppm, indicating that there are no significant interaction among the metal and these anions [10].

The complex **2·OTf·BF$_4$** is sparsely soluble in water ($S_{(H_2O)25°C}$ = 2.7 mg/cm^3) but larger than that for the earliest reported [RuCpCl(PPh$_3$)(mPTA)]·(OTf) (**3·OTf**) ($S_{(H_2O)25°C}$ = 1.1 mg/cm^3) [3] in spite of this complex includes only one PPh$_3$. This fact apparently contradicts our early supposition on the influence of the number of PPh$_3$ ligands coordinate to the metal.

To further verify the effect of the PPh$_3$ on the water solubility of this complex family, the new member [RuCp(PPh$_3$)(PTA)(mPTA)](OTf)(Cl) (**4·OTf·Cl**) was synthesized (Scheme 1). The ^{31}P{^{1}H} NMR spectrum displays an AMX system at -39.40 ppm for the PTA, at -16.18 ppm due to mPTA and at 47.22 ppm for the PPh$_3$. Compound **4·OTf·Cl** however displays a lower water solubility ($S_{(H_2O)25°C}$ = 0.4 mg/cm^3) than that of **3·OTf** (Table 2). This fact suggested that the water solubility of these complexes could be also affected by counterion salt effects and/or halide coligands.

In order to tackle this question the complex, [RuCpI(PPh$_3$)(mPTA)]·I·EtOH (**5·I·EtOH**) was synthesized from **3·OTf** (Scheme 1) where both triflate ion and chloride ligand were replaced by iodide. The composition of **5·I·EtOH** was clearly supported by the determination of its crystal structure by single crystal X-ray diffraction (Table 1 and Fig. 3). It is important to stress that **5·I·EtOH** is less soluble in water than **3·OTf** ($S_{(H_2O)25°C}$ ≤ 0.1 mg/cm^3). This behaviour, has been previously observed by us for the complexes [RuCpI(PPh$_3$)(mPTA)]·(X) ($S_{(H_2O)25°C}$: X = Cl: 0.4 mg/cm^3; X = OTf: ≤ 0.1 mg/cm^3) [3], where the decreasing solubility can be rationalized in terms of anion salt effect. Therefore, addition of NaI to **3·OTf** (Scheme 1) should provide a less water soluble complex, suggesting that I$^-$ anion exhibits a comparable effect on the solubility to than Cl$^-$ and $^-$OTf anions (Table 2).

On the other hand, this low solubility could indicate that the strategy to modify the hydrosolubility using PPh$_3$ in combination with one hydrophilic coligand in the {RuCpX(L^1)(L^2)} moiety (X =Cl, I; L^1 = PPh$_3$; L^2 = mPTA) is invalid but also it is possible that more than one water soluble ligand coordinated to the metal are required (*vide infra*).

In fact, we have found that more than one mPTA and/or PTA per ruthenium atom is enough to achieve a significant water-solubility (Table 2). For example, complex [RuCpCl(mPTA)$_2$]·(OSO$_2$CF$_3$)$_2$ ($S_{(H_2O)25°C}$ = 16 mg/cm^3) is more soluble in water than [RuCpCl(mPTA)$_2$]·(BF$_4$)$_2$ ($S_{(H_2O)22°C}$ = 0.29 mg/cm^3) [10] but surprisingly smaller than [RuCpI(mPTA)$_2$]·(OSO$_2$CF$_3$)$_2$ ($S_{(H_2O)25°C}$ = 32 mg/cm^3) [3]. The access of water molecules into the solid to interact with complex units leading to their dissolution is known to be more problematic for BF$_4^-$ salts than for $^-$OSO$_2$CF$_3$ salts. Nevertheless, this effect should not be the main reason for understand the observed solubility trend.

To understand this behaviour, the synthesis of [RuCpBr(PTA)$_2$] (**6·3.5H$_2$O**) was carried out (Scheme 1). This complex was obtained by reaction of [RuClCp(PTA)$_2$] [2,5] and KBr in refluxing methanol. Single crystals were grown by slow evaporation from its aqueous solution. The structure of **6·3.5H$_2$O** has been unequivocally confirmed by single-crystal X ray diffraction that confirms the coordination of a Br to the Ru instead of the Cl (Table 1 and Fig. 4). Its ^{31}P{^{1}H} NMR is in agreement with the observed fact that substitution of the chloride bonded to the metal by iodide causes the chemical shift of the phosphine resonances to move to higher field [3] (*vide infra*). The chemical shift of PTA in [RuClCp(PTA)$_2$] (-23.6 ppm) [2] is shifted by *ca.* 2.8 ppm up-field than that in **6·3.5H$_2$O** and shifted by *ca.* 5 ppm up-field from that [RuICp(PTA)$_2$] [3].

Compound **6·3.5H$_2$O** is less water-soluble ($S_{(H_2O)25°C}$ = 30 mg/cm^3) than [RuClCp(PTA)$_2$] [2] ($S_{(H_2O)25°C}$ = 40 mg/cm^3), slightly more soluble than [RuCp*Cl(PTA)$_2$] ($S_{(H_2O)25°C}$ = 25 mg/cm^3) [2] but much more soluble than [RuCpI(PTA)$_2$] ($S_{(H_2O)25°C}$ = 10 mg/cm^3) [3]. Therefore, as we anticipated when bromide or iodide replaces chloride the solubility in water drops down.

From above results (Table 2) it should be noted that there are a larger variety of factors than the number of water-soluble phosphines bonded to the metal, which can determine the solubility of their metal-complexes. For example, we showed that reaction of complex [RuClCp(PTA)$_2$] [2,5] in acidic media provides the larger water-soluble complex [RuClCp(HPTA)$_2$]Cl$_2$·2H$_2$O (HPTA = 1-H-1,3,5-triaza-7-phosphaadamantane) ($S_{(H_2O)25°C}$ = 320 mg/cm^3) [11]. Although, this complex is outside the scope of this paper, its high solubility is under assumption that the protonated adamantly-cage would be a major contribution to stabilization by weak intermolecular interactions and thereby increase solubility in water.

In order to complete our study, the complexes [RuCp(PTA)$_2$(mPTA)](OTf)(Cl) (**7·OTf·Cl**) and [RuCp(PTA)$_3$](BF$_4$) (**8·BF$_4$**) were obtained by replacing the Cl ligand in [RuClCp(PTA)$_2$] [2,5] with the water-soluble phosphines mPTA and PTA respectively, in presence of NaBF$_4$ (Scheme 1). This metathesis reaction was confirmed by the appearance in the ^{31}P{^{1}H} NMR of a triplet at -8.6 ppm (mPTA) in **7·OTf·Cl** and a singlet at -24.09 ppm (PTA) in **8·BF$_4$**. As expected (*vide supra*), the chemical shift of PTA in [RuClCp(PTA)$_2$] (-23.6 ppm) [2] is shifted by *ca.* 2.4 ppm up-field than that in **7·OTf·Cl**, which is closer to that in **6·3.5H$_2$O,** and shifted by *ca.* 0.5 ppm up-field from that **8·BF$_4$**. In the ^{1}H NMR spectrum of **7·OTf·Cl** the Cp chemical shift arises shifted by *ca* 0.6 ppm down-field from that observed for **8·BF$_4$** while is almost the same than that found for

2·OTf·BF$_4$. Finally, the ^{19}F{^{1}H} NMR spectrum shows that for both complexes there are no significant interaction between the metal and anions [10]. Surprisingly, **8·BF$_4$**, which contains three PTA, displays the same water-solubility ($S_{(H_2O)25°C}$ = 40 mg/cm^3) than [RuClCp(PTA)$_2$] [2,5] with only two PTA, but significantly lower than **7·OTf·Cl** ($S_{(H_2O)25°C}$ = 200 mg/cm^3) that contains one mPTA and two PTA. However, this last complex displays much more water-solubility than **4·OTf·Cl** (Table 2), which is constituted by one PTA, one mPTA and one PPh$_3$.

3.2. Crystal structures

The asymmetric unit of **3·OTf** is constituted by one triflate anion disordered by rotation around the C-S bond and the enantiomeric cationic unit [RuCpCl(PPh$_3$)(mPTA)]$^+$.

Selected distances and angles are collected in Table 3. The ruthenium atom is coordinated with a pseudo-octahedral geometry to one η^5-Cp, formally occupying three contiguous coordination positions, one Cl, one PPh$_3$ and one mPTA. Actuation of the symmetry element (-1) leads to the enantiomeric unit (Fig. 2) and, therefore, **3·OTf** is a racemate constituted by the two possible enantiomers obtained by distribution of the four different ligands around the Ru atom.

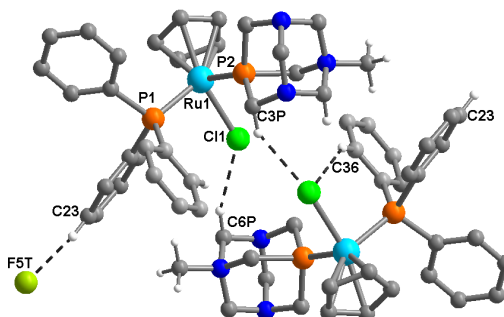**Fig. 2**. A perspective drawing of **3·OTf** with atom numbering. Dashed lines represent the select inter-molecular interactions.

The P1-Ru1-P2 angle is found to be 99.02(10)°, in line to that found in [RuCpCl(PPh$_3$)(PTA)] (mean 98.99(8)°) [3] and slightly higher than in [RuClCp(PPh$_3$)(dmoPTA)]$^+$ 98.37(9)°) [12]. The Cp ring is essentially planar, the biggest separation being 0.017 Å (C1).

The Ru-Cp$_{centroid}$ distance is 1.839 Å, comparable with that for those complexes earliest report containing PTA (mean 1.847 Å) [3] and dmoPTA (1.860 Å) [12]. The Ru-P$_{mPTA}$ separation (Ru1-P2 = 2.261(3) Å) match closely to that found in [RuClCp(mPTA)$_2$]$^{2+}$ (mean 2.255(12) Å) [10] but is shorter than in [RuClCp(PPh$_3$)(dmoPTA)]$^+$ (2.277(3) Å) [12].

The Ru-Cl distance (2.447(3) Å) in line with to the average value (medium: Ru-Cl = 2.447(7) Å) found in bibliography [2,3,5,10,11,12].

Selected distances and angles for **5·I·EtOH** are displayed in Table 3. The asymmetric unit of crystal structure of this complex is constituted by a chiral molecule containing a metal coordinated to a Cp, a PPh$_3$, an iodide and a mPTA coordinated by the P (Fig. 3).

We must note that, compound **5·I·EtOH** is constituted by the same complex but different counter ions than [RuCpI(PPh$_3$)(mPTA)]·(OSO$_2$CF$_3$)·2H$_2$O, which was previously described by us [3]. This last compound crystallises in the monoclinic system (P2$_1$/c space group), while compound **5·I·EtOH** crystallises in the triclinic system (P-1 space group).
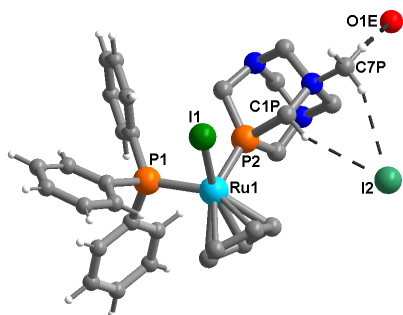
The geometry of the complex is quite similar to that of **3·OTf** discussed previously. The Cp ring is practically planar with the larger separation from the overal Cp plane of only 0.0085 Å (C5). The Ru-Cp$_{centroid}$ distance (1.851 Å) is consistent with the values reported for [RuCpI(PPh$_3$)(PTA)] (1.852 Å) and [RuCpI(PPh$_3$)(mPTA)]$^+$ (1.8563(7) Å) [3].

The coordination P1-Ru1-P2 angle, is found to be 99.42(4)°, which is slightly shorter than in [RuCpI(PPh$_3$)(mPTA)]$^+$ (100.12(8)°) and *ca.* 2.1° greater than that found for [RuCpI(PPh$_3$)(PTA)]$^+$ (97.31(4)°) [3]. This fact suggests that the steric interactions are similar in both complexes.

The Ru-I distance in **5·I·EtOH** (2.7164(4) Å shortened respecting to [RuCpI(PPh$_3$)(PTA)]$^+$ (2.7514(4) Å) but, match closely to that found in [RuCpI(PPh$_3$)(mPTA)]$^+$ (2.724 Å) as well as to the mean value (2.711 Å) for the known [CpRuIL$_2$] complex structures [3].

The crystal structure of **6·3.5H$_2$O** is constituted by a achiral unit [RuCpBr(PTA)$_2$] made by a ruthenium coordinated to a η^5-Cp, a Br and two PTA bonded by the P atom. A perspective drawing is shown in Fig. 4 and selected distances and angles in Table 3.

The coordination polyhedron about the metal atom adopts a highly distorted pseudo-octahedral geometry (P1-Ru1-P2 = 98.13(6)°). This angle value is larger than that found for [RuClCp′(L$_2$)] (Cp′= Cp, Cp*; L$_2$ = PTA; HPTA) (93.30(5)-96.85(5)°, mean 95.44(6)°) [2,5,11] and shorter than [RuClCp(mPTA)$_2$]$^{2+}$ (99.44(4)°) [10]. This result is intriguing due to the larger size of bromide that, likely increases the repulsion between the halide ligand and the other coordinated ligands.

These observations are consistent with the greater steric and electrodonating properties of PPh$_3$ versus PTA-derivatives and Cp* versus Cp, which should have anticipated dissimilar intramolecular repulsions in related piano-stool complexes [3,5].

Another important metrical characteristic are as follows: The Cp ring is practically planar with the larger separation from the overall Cp plane of only 0.0035 Å (C34). The Ru-Cp$_{centroid}$ distance (1.849 Å) comparable with the values found in bibliography (range 1.840-1.861 Å, median: 1.849 Å) [3,10,11]. The Ru-Br distance (2.5832(7) Å), identical to those found for the Ru(II)-aminophosphine complexes [RuCp-(PN-κN,κP)(CH$_3$CN)]$^+$ (2.589(2) Å) [13].
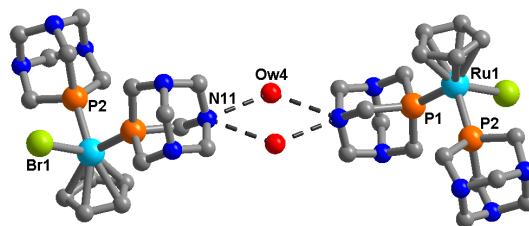
Table 3. Selected distances (Å) and angles (º) for **3·OTf**, **5·I·EtOH** and **6·3.5H₂O**

3·OTf

Ru-P1	2.300(3)
Ru-P2	2.261(3)
Ru-Cl1	2.447(3)
Ru-Cp$_{centroid}$	1.839
P2-Ru-P1	99.02(10)
P1-Ru-Cl1	90.96(9)
P2-Ru-Cl1	87.60(9)

5·I·EtOH

Ru-P1	2.3077(10)
Ru-P2	2.2609(10)
Ru-I1	2.7164(4)
Ru-Cp$_{centroid}$	1.851
P2-Ru-P1	99.42(4)
P1-Ru-I1	90.75(3)
P2-Ru-I1	87.72(3)

6·3.5H₂O

Ru1-P1	2.2587(16)
Ru1-P2	2.2644(17)
Ru1-Br1	2.5832(7)
Ru-Cp$_{centroid}$	1.849
P1-Ru1-P2	98.13(6)
P1-Ru1-Br1	91.01(4)
P2-Ru1-Br1	89.21(4)

Table 4. Additional weak intermolecular interactions for **3·OTf**, **5·I·EtOH** and **6·3.5H₂O**. D and A stand for donor and acceptor, respectively.

D-H···A	D···A (Å)	H···A (Å)
3·OTf		
C3P-H3P1····Cl1	3.738(1)	2.850(3)
C6P-H6P2····Cl1	3.687(2)	2.762(3)
C36-H36······Cl1	3.633(1)	2.843(3)
5·I·EtOH		
C1P-H1PA····I1	3.562(5)	2.947(3)
C2-H2····I1	3.828(4)	3.115(3)
C3P-H3PB····I1	3.905(3)	3.018(3)
C6P-H6PA····I1	3.880(4)	2.990(3)
C2P-H2PB····I2	3.935(4)	3.211(3)
C4P-H4PB····I2	4.074(4)	3.197(3)
C24-H24······I2	4.051(5)	3.311(3)
O1E·······I2	3.484(4)	--
C7P-H7PB···O1E	3.449(8)	2.560(5)
6·3.5H₂O		
C12-H12B·····Ow1	3.634(7)	2.696(4)
C14-H14A·····Ow1	3.835(8)	2.950(4)
C34-H34·······Ow1	3.610(8)	2.684(4)
C35-H35·······Ow1	3.532(7)	2.947(4)
N13·····Ow1	2.827(7)	
C35-H35·······Ow2	3.270(8)	2.713(4)
C14-H14A·····Ow2	3.384(7)	2.762(4)
C24-H24B·····Ow2	3.228(8)	2.852(5)
C31-H31·······Ow2	3.664(9)	2.894(5)
C13-H13B·····Ow2	3.537(7)	2.805(4)
N23·····Ow2	2.898(6)	--
C13-H13B·····Ow3	3.774(9)	2.811(5)
C22-H22A·····Ow3	3.601(8)	2.671(5)
C32-H32·······Ow3	3.554(9)	2.704(7)
Br1·····Ow3	3.327(6)	--
C25-H25A·····Ow4	3.286(1)	2.803(9)

Figs. 2 and 3 show a perspective view of the crystal packing for **3·OTf** and **5·I·EtOH**, respectively. The disordered triflate anion and ethanol molecules, respectively, have been interspersed in the lattice, clearly located between the C23-H23····F5T (2.554(3) Å) for **3·OTf** and C7P-H7PB····O1E (2.560(5) Å) and C4P-H4PA····O1E (2.417(5) Å) for **5·I·EtOH**.

It is also worth mentioned that in this complex the iodide counterions are all anchored through hydrogen-bonding interactions C1P-H1PB····I2 (3.052(2) Å) and C7P-H7PC····I2 (3.061(3) Å).

The structure of the compound **6·3.5H₂O** (Fig. 4) can be visualised as two achiral units [RuCpBr(PTA)₂] linked in the μ_2-Ow4. The Ow4-N11 distances through this bridging are: 2.790(2) Å for N11 (1-x, 0.5+y, 0.5-z) and 2.890(1) Å for N11 (x, 0.5-y, -0.5+z).

Likewise, in the crystal packing diagrams from the three complexes another weak intermolecular interaction provides additional stabilization of their crystal structure (Table 4).

characterization of a new member of the piano-stool family [RuCpX(L^1)(L^2)]$^{n+}$ (X = Cl⁻, Br⁻, I⁻; L^1 = PPh₃; mTPPMS, L^2 = mPTA, PTA; L^1 = L^2 = PTA, mPTA) have been presented. The comparison of the composition and water solubility of the family members suggested some relationship between water solubility and complex composition.

All IR and NMR analyses supported the proposed composition for the new complexes and indicate that their solid state structure is maintained in solution.

4. Conclusions

In this overview, the synthesis and structural

The combination of PPh$_3$ and mTPPMS phosphanes shows that the steric and electronic properties cannot be regarded as separated factors and both influence the complex water-solubility. Likewise, the incorporation of two PTA with one mPTA in the {RuCp} moiety, met with greater success in the complex **7·OTf·Cl**, the most water-soluble complex tested. The incorporation of two PTA in the {RuCpX} moiety (X = Cl, Br, I) becomes more soluble as the ionic radii of halide ligand decreases.

Acknowledgments

Supplementary material

X-ray crystallographic data of complexes **3·OTf** (CCDC 1475100); **5·I·EtOH** (CCDC 1475101) and **6·3H$_2$O** (CCDC 1475102) (CIF). These data can be obtained free of charge from the Cambridge Crystallographic Data Centre via www.ccdc.cam.ac.uk.data-request/cif.

References

[1] (a) For an historial overwiews on *HSAB Priciple*, see: R.G. Pearson, J. Am. Chem. Soc., 85 (1963), 3533; R.G. Pearson, Inorg. Chim. Acta 240 (1995) 93 and R.G. Pearson, Struct Bond., 80 (1993) 1.
  (b) R.G. Pearson, Acc. Chem. Res., 26 (1993) 250; R.G. Pearson, J. Am. Chem. Soc., 110 (1988) 7684; R.G. Pearson, J. Chem. Educ., 45 (1968), 581; R.G. Pearson, J. Chem. Educ. 45 (1968) 643.

[2] D. N. Akbayeva, L. Gonsalvi, W. Oberhauser, M. Peruini, F. Vizza, P. Brüggeller, A. Romerosa, G. Sava, A. Bergamo, Chem Commun., (2003) 264 and references therein.

[3] A. Romerosa, T. Campos-Malpartida, C. Lidrissi, M. Saoud, M. Serrano-Ruiz, M. Peruzzini, J. A. Garrido-Cárdenas, F. García-Moroto, Inorg. Chem., 45 (2006) 1289 and references therein.

[4] A. Romerosa, M. Saoud, T. Campos-Malpartida, C. Lidrissi, M. Serrano-Ruiz, M. Peruzzini, J. Antonio-Garrido, F. García-Moroto, Eur. J. Inorg. Chem., (2007) 2803 and references therein.

[5] B. J. Frost, C. A. Mebi, Organometallics, 23 (2004) 5317.

[6] G. Sheldrick, Acta Crystallogr. A64 (2008) 112.

[7] K. Vikse, G.N. Khairallah, J.S. Mclndoe, R. A. J. O´Hair, Dalton Trans., 42 (2013) 6440.

[8] (a) E. Negishi, A. de Meijere (Eds.) Handbook of Organopalladium Chemistry for Organic Synthesis, Wiley-Interscience, 2002, p. 2965;
  (b) N. Pinault, D.W. Bruce, Coord. Chem. Rev., 241 (2003) 1;
  (c) J. J Spivey (Ed.) Specialist Periodical Reports Catalysis: Volume 13, The Royal Society of Chemistry, 1997, 117.

[9] A. D. Phillips, L. Gonsalvi, A. Romeros, F. Vizza, M. Pruzzini, Coord. Chem. Rev., 248 (2004) 955.

[10] B. González, P. Lorenzo-Luis, P. Gili, A. Romerosa, M. Serrano-Ruiz, J. of Organometallic Chem., 694 (2009) 2029.

[11] M. Serrano-Ruiz, P. Lorenzo-Luis, A. Romerosa, A. Mena-Cruz, Dalton Trans., 42 (2013) 7622.

[12] Mena-Cruz, P. Lorenzo-Luis, A. Romerosa, M. Saoud, M. Serrano-Ruiz, Inorg. Chem., 46 (2007) 6120.

[13] C. Standfest-Hauser, C. Slugovc, K. Mereiter, R. Schmid, K. Kirchner, L. Xiao, W. Weissensteiner, Dalton Trans., (2001) 2989.